Equilibrium Analyses of the Active-Site Asymmetry in Enterococcal NADH Oxidase: Role of the Cysteine-sulfenic Acid Redox Center†

T. Conn Mallett, Derek Parsonage, and Al Claiborne*

Department of Biochemistry, Wake Forest University Medical Center, Winston-Salem, North Carolina 27157

Received July 22, 1998; Revised Manuscript Received December 21, 1998

ABSTRACT: Recent studies [Mallett, T. C., and Claiborne, A. (1998) *Biochemistry 37*, 8790−8802] of the O_2 reactivity of C42S NADH oxidase ($O_2 \rightarrow H_2O_2$) revealed an asymmetric mechanism in which the two $FADH_2$·NAD^+ per reduced dimer display kinetic inequivalence. In this report we provide evidence indicating that the fully active, recombinant wild-type oxidase ($O_2 \rightarrow 2H_2O$) displays thermodynamic inequivalence between the two active sites per dimer. Using NADPH to generate the free reduced wild-type enzyme (EH_2'/EH_4), we have shown that NAD^+ titrations lead to differential behavior as only one $FADH_2$ per dimer binds NAD^+ tightly to give the charge-transfer complex. The second $FADH_2$, in contrast, transfers its electrons to the single Cys42-sulfenic acid (Cys42-SOH) redox center, which remains oxidized during the reductive titration. Titrations of the reduced NADH oxidase with oxidized 3-acetylpyridine and 3-aminopyridine adenine dinucleotides further support the conclusion that the two $FADH_2$ per dimer in wild-type enzyme can be described as distinct "charge-transfer" and "electron-transfer" sites, with the latter site giving rise to either intramolecular (Cys42-SOH) or bimolecular (pyridine nucleotide) reduction. The reduced C42S mutant is not capable of intramolecular electron transfer on binding pyridine nucleotides, thus confirming that the Cys42-SOH center is in fact the source of the redox asymmetry observed with wild-type oxidase. These observations on the role of Cys42-SOH in the expression of thermodynamic inequivalence as observed in wild-type NADH oxidase complement the previously described kinetic inequivalence of the C42S mutant; taken together, these results provide the overlapping framework for an alternating sites cooperativity model of oxidase action.

In the heme- and cytochrome-deficient enterococci and streptococci, the flavoprotein NADH oxidase (Nox)[1] catalyzes the direct four-electron reduction of $O_2 \rightarrow 2H_2O$ (*1*, *2*). In so doing, this unusual enzyme helps to provide an intracellular NAD^+/NADH balance which is optimal for glycolysis (*3*); at the same time, by avoiding one-electron (→superoxide) and two-electron (→H_2O_2) reductions of O_2, Nox contributes significantly to the antioxidant defense mechanisms of these bacteria (*4*). The enzyme has been purified from *Enterococcus faecalis* (*1)* and *Streptococcus mutans* (*5*); the *E. faecalis* Nox is a dimer of two identical 50 kDa subunits. In addition to FAD, each subunit contains a stabilized sulfenic acid derivative of Cys42 (Cys42-SOH; ref *1*); the essential role of this non-flavin redox center has been analyzed in detail in the closely related NADH peroxidase (Npx; refs *6*−*8*). Recent kinetic analysis of a C42S Nox mutant lacking this redox center (*9*) has shown that the enzyme now catalyzes the two-electron reduction of $O_2 \rightarrow H_2O_2$, confirming the essential catalytic redox role of Cys42-SOH/Cys42-SH in the reduction of $O_2 \rightarrow 2H_2O$, as well.

Working with the wild-type Nox as originally purified from *Streptococcus* (now *Enterococcus) faecalis* 10C1, reductive titrations with dithionite and NADH repeatedly were shown to require 1.5−1.6 equiv of reductant per FAD (*1*, *2*) as opposed to the expected stoichiometry of 2 equiv of reductant per FAD. Still both FAD on each monomer were reduced completely, and the earlier analysis (*2*) focused on the Cys42-SOH redox center as the source of the inequivalence observed under equilibrium conditions for the two active sites per dimer. Further evidence for this active-site asymmetry came from titrations of the dithionite-reduced wild-type enzyme with NAD^+ and with the nonreducible analogue AAD^+. In each case one $FADH_2$ per reduced dimer (1.14 $FADH_2$ with NAD^+ and 1.0 $FADH_2$ with AAD^+) was reoxidized anaerobically at pH 7.0 on titration with the pyridine nucleotide; with NAD^+ it was clear that intermolecular electron transfer ($NAD^+ \rightarrow$ NADH) was not significant. These observations led to the conclusion that the one Cys42-SOH per dimer remaining in dithionite-reduced Nox could accept two electrons directly from its active-site

† This work was supported by National Institutes of Health Grant GM-35394.

* To whom correspondence should be addressed. Tel: (336) 716-3914. Fax: (336) 716-7671. URL: http://invader.bgsm.wfu.edu/.

[1] Abbreviations: Nox, NADH oxidase; Cys42-SOH, Cys42-sulfenic acid; AAD^+, 3-aminopyridine adenine dinucleotide; E, oxidized enzyme; $AcPyAD^+$, 3-acetylpyridine adenine dinucleotide (oxidized); AcPyADH, 3-acetylpyridine adenine dinucleotide (reduced); IPTG, isopropyl β-D-thiogalactopyranoside; DTT, dithiothreitol; PCR, polymerase chain reaction; TYP, tryptone−yeast extract−phosphate medium; SDS−PAGE, sodium dodecyl sulfate−polyacrylamide gel electrophoresis; E'^0, midpoint oxidation−reduction potential (E_m) at pH 7.0; EH_2, two-electron reduced enzyme (FAD, Cys42-SH); CHES, 2-(*N*-cyclohexylamino)ethanesulfonic acid; EH_2', two-electron reduced enzyme ($FADH_2$, Cys42-SOH); EH_4, four-electron reduced enzyme ($FADH_2$, Cys42-SH); E_h, calculated system potential; Npx, NADH peroxidase; LipDH, lipoamide dehydrogenase; MR, mercuric reductase; EHR, reduced monoalkylated enzyme; GR, glutathione reductase; $AADP^+$, 3-aminopyridine adenine dinucleotide phosphate.

10.1021/bi9817717 CCC: $18.00
Published on Web 02/19/1999

Scheme 1

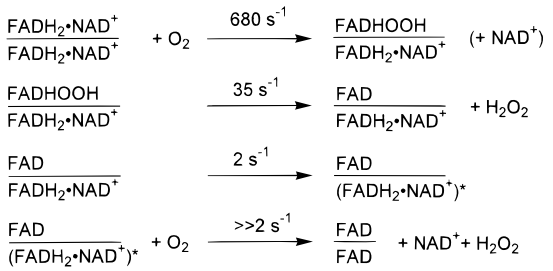

$FADH_2$ redox partner on binding NAD^+ or AAD^+. With NAD^+, this process of intramolecular electron transfer was proposed (*2*) to involve a pyridine nucleotide binding site distinct from that involved in stable formation of the $E-FADH_2 \cdot NAD^+$ charge-transfer complex, which was also observed.

The availability of the C42S Nox mutant made a direct test of this idea possible, and the potential relevance of this active-site asymmetry as observed under equilibrium conditions to the catalytic redox mechanism of wild-type Nox added to the significance of this study. We have recently shown (*9*) that an asymmetric kinetic mechanism, consistent with an alternating sites cooperativity model (*10*), applies for the O_2 reactivity of the reduced C42S $Nox \cdot NAD^+$ complex; the reaction proceeds with the intermediate formation of an FAD C(4a)-hydroperoxide which eliminates H_2O_2 to regenerate the oxidized E−FAD form. However, full reoxidation of one $FADH_2$ per dimer is necessary before O_2 can react with the second $FADH_2$, and a rate-limiting step of 2 s^{-1} attributed to a change in protein conformation couples the respective O_2 reactions of the two subunits per dimer (see Scheme 1). In view of the kinetic inequivalence expressed by the reduced C42S $Nox \cdot NAD^+$ complex on reaction with O_2, we therefore decided to investigate the interactions of pyridine nucleotides with both recombinant wild-type and C42S Nox under equilibrium conditions.

EXPERIMENTAL PROCEDURES

Materials. NADH, NAD^+, and NADPH were purchased from Boehringer Mannheim, and AcPyADH, $AcPyAD^+$, and AAD^+ were from Sigma. IPTG was purchased from Ambion, and DTT was from Research Organics. 1-Deazariboflavin was the generous gift of Dr. Wallace Ashton, Merck, Sharp, and Dohme Research Laboratories. All other chemicals and restriction enzymes, as purchased from sources described previously (*2*, *9*, *11*), were of the best grades available.

Construction of a Low-Copy T7 Expression Vector, pOXO7. Expression of the wild-type *nox* gene from a high-copy T7 vector (pNOX7; ref *12*), prior to IPTG induction, limits the growth of recombinant *Escherichia coli* JM109DE3 under vigorous aeration. We therefore prepared a general low-copy T7 vector by replacing the pUC origin of replication in pOXO4 (*13*) with the p15A *ori* from pACYC184 to generate pOXO7. A *Xho*I restriction site and a consensus ribosome-binding site were introduced upstream of the *nox* coding sequence by PCR amplification of the 5′-end of the gene. The reconstructed wild-type *nox* gene including the new ribosome-binding site was subcloned into pOXO7 as a *Xho*I/*Sac*I fragment to generate the pNOX11 expression plasmid. The *Xho*I/*Hin*dIII fragment encoding the N-terminal 165 residues was subcloned into pBluescript II SK(+) and used as a template for Cys42 → Ser mutagenesis, using the Sculptor kit (Amersham). After the presence of this single mutation was confirmed, the *Xho*I/*Hin*dIII fragment was used to replace the corresponding wild-type segment in pNOX11.

Expression and Purification of Wild-Type and C42S Noxs. For the recombinant wild-type Nox, *E. coli* JM109DE3 transformed with pNOX11 was grown in 10 2.8-L Fernbach flasks, each containing 0.66 L of TYP medium plus 25 μg/mL chloramphenicol (*13*). Flasks were shaken vigorously at 37 °C until the cultures reached A600 = 1.0, and 0.4 mM IPTG was added at that time. After 4 h of induction cells were harvested and washed in 0.1 M potassium phosphate, pH 7.0, plus 1 mM EDTA and 2 mM DTT; the cell suspension was then disrupted by passage through an SLM/Aminco French press. After centrifugation of the crude extract, nucleic acids were precipitated with 2.5% (w/v) streptomycin sulfate; the 30% saturated ammonium sulfate (as defined at 25 °C) supernatant was then incubated with 62 mM DTT and 90 μM FAD at 37 °C for 5 min, a process which is intended to reconstitute any deflavo-Nox which may be present (*1*, *14*). After being filtered, the solution was loaded onto a 50-mL Phenyl Sepharose 6 Fast Flow (Pharmacia Biotech) column equilibrated with the phosphate/EDTA/DTT buffer plus 30% ammonium sulfate. The column was washed with the equilibration buffer until A280 <0.1 was reached; a 0.5-L gradient from 30% → 0 ammonium sulfate was then used to elute the enzyme. Fractions with A448 >0.1 were pooled and dialyzed twice against 4 L of 0.1 M Tris-HCl, pH 7.5 (as measured at 25 °C), containing 1 mM EDTA and 2 mM DTT, before being loaded onto a 25-mL Q Sepharose Fast Flow column equilibrated with the same buffer. After extensive washing the enzyme was eluted with a 0 → 0.5 M NaCl gradient, and fractions with A280/A448 <20 were pooled, brought to 65% ammonium sulfate, and centrifuged. The protein pellet was resuspended in 10 mL of 10 mM phosphate, pH 7.0, containing 2 mM DTT and 1 μM FAD, before being dialyzed twice against 4 L of the same buffer. The dialyzed protein was incubated (as before) with 62 mM DTT and 0.5 mM FAD at 37 °C for 5 min, centrifuged briefly, and applied to a 50-mL column of Macro-Prep Ceramic Hydroxyapatite (type 1, 40 μm; Bio-Rad Laboratories) equilibrated with the phosphate/DTT/FAD buffer. After the column was washed, the enzyme was eluted with a gradient of 10 → 40 mM phosphate, pH 7.0, containing 2 mM DTT plus 1 μM FAD. Fractions with A280/A448 <8, and which were homogeneous by SDS−PAGE, were pooled, concentrated, and buffer-exchanged by ultrafiltration into 0.1 M phosphate, pH 7.0, containing 1 mM EDTA, 2 mM DTT, and 1 μM FAD. The pure enzyme was then concentrated to 10 mg/mL in the same buffer plus 20% (v/v) glycerol; 0.2−1 mL aliquots were then flash-frozen in liquid nitrogen before being stored at −80 °C. For the wild-type enzyme in particular, the entire purification protocol was routinely completed within 24 h; all steps were carried out at 4 °C.

The preparation of the C42S mutant followed the same protocol with the following changes: (1) no reconstitution step was included prior to Phenyl Sepharose or hydroxyapatite chromatography, (2) the A280/A438 ratio of the purified mutant is 5.2, and (3) the mutant was simply stored at 4 °C as a 65% ammonium sulfate slurry in 50 mM

phosphate, pH 7.0, containing 0.5 mM EDTA and 2 mM DTT, plus 1 μM FAD.

General Procedures. Nox assays and anaerobic titrations followed established protocols (*1, 2, 9*); absorbance and fluorescence data were collected using Hewlett-Packard Model 8451A and 8452A and SLM Aminco-Bowman Series 2 instruments, respectively. E'^0 values for the FAD/$FADH_2$ redox couples in both recombinant wild-type and C42S mutant Noxs were determined by dithionite titration (*15*) in the presence of the reference dye 1-deazariboflavin ($E'^0 = -280$ mV; ref *16*), using methyl viologen at low concentration to ensure rapid equilibration of reducing equivalents. Static titrations of reduced wild-type and C42S Noxs were analyzed using the ENZFITTER program (*17*).

RESULTS

Purification and Stabilization of Recombinant Wild-Type Nox. The expression and purification protocol described in Experimental Procedures routinely yields 140−150 mg of pure enzyme (E/EH_2 form) from 6.6 L of recombinant *E. coli* cultures. In earlier studies with the enzyme purified from *E. faecalis*, a specific activity of 340 units/mg was reported; in some preparations, and for reasons that were not fully understood, specific activities of 600−700 units/mg were observed (*1*). This high-activity form of Nox was extremely labile, however. Subsequent work with the deflavo-Nox isolated from *E. faecalis* demonstrated that the enzyme activity measured on reconstitution was equivalent to a specific activity of 670−780 units/mg (*14*), similar to that of the high-activity Nox form. Recombinant Nox, in comparison, has a specific activity of 560−580 units/mg. As reported earlier (*1, 2*), the purified holo-Nox is generally quite labile on storage at either 4 or −20 °C, even in the presence of DTT. For example, when stored at 4 °C as a 65% ammonium sulfate slurry with 2 mM DTT plus EDTA and FAD, the recombinant enzyme loses 50% activity in 2 weeks. In addition to developing a purification protocol that can be completed within 24 h, we have also established a procedure which allows storage of the pure enzyme for up to 6 months with no activity loss. The concentrated protein (10 mg/mL), in 0.1 M potassium phosphate, pH 7.0, plus 20% (v/v) glycerol, 1 mM EDTA, 2 mM DTT, and 1 μM FAD, is flash-frozen in liquid nitrogen in 0.2−1 mL aliquots and stored at −80 °C.

Prior to experimental work at pH 7.0 the enzyme was diluted with 0.1 M phosphate, pH 7.0, plus 1 mM EDTA and 2 mM DTT, and concentrated with a CM-30 microconcentrator (Amicon). Since the enzyme is purified in the E/EH_2 form (*9*), it was necessary to reoxidize the EH_2 component to give the fully oxidized, resting E form. This was accomplished by spectral titration of the enzyme with 17 equiv of H_2O_2 per FAD, followed by two more CM-30 steps. The enzyme was brought up in the phosphate/EDTA/DTT buffer and used directly in titration experiments. For work at pH 8.7, early results showed that 2 mM DTT quickly reduced E → E/EH_2, so the enzyme was simply taken through three CM-30 steps with the pH 7.0 buffer before the final concentrated protein was diluted directly with 0.1 M CHES, pH 8.7, containing 1 mM EDTA and 2 mM DTT. Enzyme activity was carefully monitored before and after titration experiments at pH 7.0 and 8.7, and essentially no activity losses were observed.

Scheme 2

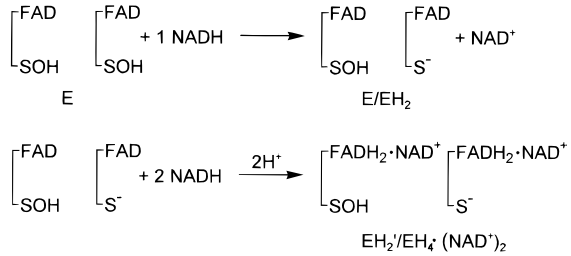

The expression and purification protocol for the Nox C42S mutant routinely gave 40 mg of enzyme from 6.6 L of *E. coli*, and the stability of this protein allowed it to be stored as a 65% ammonium sulfate slurry at 4 °C with no significant activity loss. The catalytic properties have recently been described (*9*); the mutant specific activity is 16−20 units/mg, and the enzyme catalyzes the stoichiometric reduction of $O_2 \rightarrow H_2O_2$ with 1 equiv of NADH. Initial experiments with the mutant included 2 mM DTT as a precaution, but DTT has no effect on activity or stability and was later eliminated in work with C42S Nox. The enzyme was prepared for experiments by CM-30 concentration and buffer exchange into 50 mM phosphate, pH 7.0, plus 0.5 mM EDTA.

The spectral and fluorescence properties of the wild-type E/EH_2 and C42S Nox forms have recently been described (*9*).

Redox Properties of Wild-Type Nox at pH 7.0: Titrations with NADPH and NAD^+. Reductive titrations of wild-type Nox purified from *E. faecalis* consistently give stoichiometries of 1.5−1.7 equiv of dithionite or NADH per FAD (*1, 2, 14*), and this behavior has been interpreted in terms of active-site asymmetry within the dimeric Nox (see Scheme 2). Only one of the two Cys42-SOH redox centers per dimer is reduced; the first phase of reduction gives the E/EH_2 form, and full reduction with NADH yields the $EH_2'/EH_4{\cdot}(NAD^+)_2$ species (*2*). Recombinant wild-type Nox exhibits virtually identical behavior in titrations with both dithionite and NADH, which also give stoichiometries of 1.4−1.5 equiv of reductant per FAD, and the reduced enzyme·NAD^+ complex exhibits a long-wavelength charge-transfer band centered at 720 nm. We have shown that when the closely related NADH peroxidase is reduced with NADPH instead of NADH, the analogous charge-transfer band is absent (*18*). Figure 1 gives the result of an anaerobic titration of wild-type Nox with NADPH at pH 7.0. The first phase is identical to those seen with dithionite or NADH and corresponds to the reduction of E → E/EH_2 with 0.46 equiv of NADPH per FAD. It is important to emphasize that this stoichiometry is the same as that represented (one NADH per dimer) in the first step of Scheme 2. While the second phase does correspond to addition of 1.1 equiv of NADPH and yields the EH_2'/EH_4 form with both FAD on each monomer reduced, there is absolutely no development of long-wavelength absorbance. The conclusion from this titration is that although NADPH can reduce Nox in a manner directly comparable to NADH, the $NADP^+$ product is not bound by the reduced enzyme.

In an earlier report (*2*) we demonstrated that NAD^+ titration of dithionite-reduced Nox at pH 7.0 led to reoxidation of one $FADH_2$ per dimer (57% observed) at the

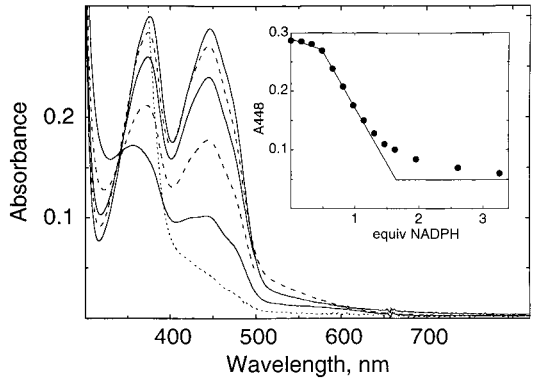

FIGURE 1: Anaerobic titration of recombinant wild-type Nox with NADPH at pH 7.0. The anaerobic cuvette contained 1.0 mL of 24.9 μM enzyme (FAD) in the phosphate/EDTA/DTT buffer. Spectra shown in order of decreasing A448 correspond to oxidized enzyme (E; —), and enzyme after addition of 0.49 (E/EH_2; - - -), 0.65 (—), 0.98 (- - -), 1.47 (—), and 6.52 (EH_2'/EH_4; ···) equiv of NADPH/FAD. Inset: Absorbance change at 448 nm versus added NADPH. The end points correspond to 0.46 and 1.6 equiv of NADPH/FAD. The oxygen-scrubbing system consisting of protocatechuate dioxygenase and protocatechuic acid was added anaerobically prior to the titration.

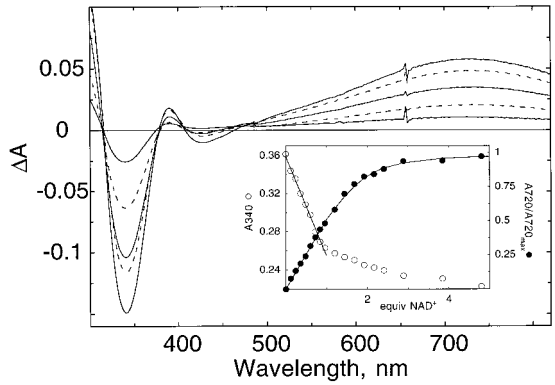

FIGURE 2: Titration of the wild-type Nox EH_2'/EH_4 form with NAD^+ at pH 7.0. An enzyme solution (1.0 mL) containing 28 μM Nox in the phosphate/EDTA/DTT buffer was reduced with 2.8 equiv of NADPH/FAD. After the NADPH syringe was exchanged for one containing 2.33 mM NAD^+, the titration was continued. Difference spectra (minus free reduced enzyme) shown in order of increasing A720 represent complexed enzyme after addition of 0.36 (—), 0.72 (- - -), 1.2 (—), 2.4 (- - -), and 7.2 (—) equiv of $NAD^+/FADH_2$. Inset: Absorbance changes at 340 and 720 nm versus added NAD^+.

expense of the remaining Cys42-SOH. More recent work with dithionite-reduced C42S Nox (*9*), however, demonstrated the formation of an NAD^+—sulfite adduct similar to that described by Pfleiderer et al. (*19*). This adduct is recognized by its near-UV absorbance maximum of about 320 nm, but more importantly it complicates both the spectral and chemical courses of NAD^+ titration of reduced C42S Nox as well as the accurate determination of free [NAD^+]. The results given in Figures 1 and 2 suggest that NAD^+ titration of NADPH-reduced Nox might circumvent the problems associated with dithionite reduction, but it should be noted that complete reduction of Nox at pH 7.0 requires the addition of approximately 3 equiv of NADPH. When NAD^+ is titrated anaerobically into a solution of the Nox EH_2'/EH_4 form containing excess NADPH (Figure 2), the primary observation is the appearance of the E—$FADH_2$·NAD^+ charge-transfer band over the range 490—820 nm;

Scheme 3

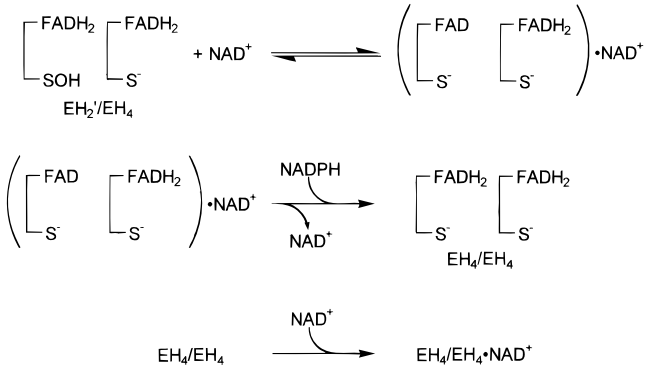

formation of this complex is not inhibited by the 1.2 equiv of $NADP^+$ present, again confirming the absence of any E—$FADH_2$·$NADP^+$ interaction. The flavin components of both subunits (EH_2'/EH_4) remain fully reduced throughout the NAD^+ titration, although perturbations in the E—$FADH_2$ spectrum are observed which give rise to apparent isosbestic points at 380, 405, and 486 nm. The decrease in A340, which is observed as a strictly linear function of equivalents of NAD^+ added until 50% of the E—$FADH_2$·NAD^+ complex (as measured at 720 nm) is formed, is equivalent to the oxidation of 0.58 mol of NADPH/FAD over the range 0—1 equiv NAD^+. The increase in A720 is also strictly linear through this [NAD^+] range; this absorbance change is observed as the consequence of at least three specific enzyme events. First, added NAD^+ must bind to the EH_2'/EH_4 dimer; this event leads to intramolecular electron transfer within the EH_2' subunit ($FADH_2$ → Cys42-SOH), yielding the EH_2'/EH_4 dimer (see Scheme 3). The nascent oxidized FAD of the EH_2 monomer is then (readily) reduced by the excess NADPH present; if we presume the first NAD^+ binds the original EH_2' subunit directly, this NAD^+ must also dissociate prior to NADPH reduction. Finally, the EH_4/EH_4 dimer which results binds free NAD^+, giving rise to the A720 increase measured experimentally under equilibrium conditions. The linear decrease in A340 described above represents the associated oxidation of one NADPH per dimer (0.5 equiv of NADPH per FAD). Given the strictly linear increase in A720 during this phase of the titration, it appears that the apparent K_d for NAD^+ binding is $\ll 1$ μM.

Once this phase (corresponding to 1 NAD^+ added per $FADH_2$) is complete, the enzyme consists of a homogeneous (EH_4/EH_4)·NAD^+ population. Subsequent addition of NAD^+ in the range 1—5 equiv per $FADH_2$ leads directly to the saturable A720 increase observed, without the associated redox chemistry and NAD^+ dissociation events intrinsic to the A720 change in the preceding phase. There is little or no decrease in A340 during the second phase, which adds further support to this interpretation. The 720 nm data set over this [NAD^+] range corresponds to a simple, reversible binding process with a stoichiometry of one NAD^+ per $FADH_2$ and a K_d of 5.4 μM. On completion of the titration the fully formed EH_4·NAD^+ complex is present; the ϵ720 value of 1920 M^{-1} cm^{-1} is comparable to that (2360 M^{-1} cm^{-1}) resulting from direct NADH titration at pH 7.0 and could reflect intrinsic differences between the EH_2'/EH_4·$(NAD^+)_2$ and EH_4·NAD^+ forms.

Redox Potential for the Wild-Type Nox E/EH₂ Form. One factor which could contribute to the active-site asymmetry

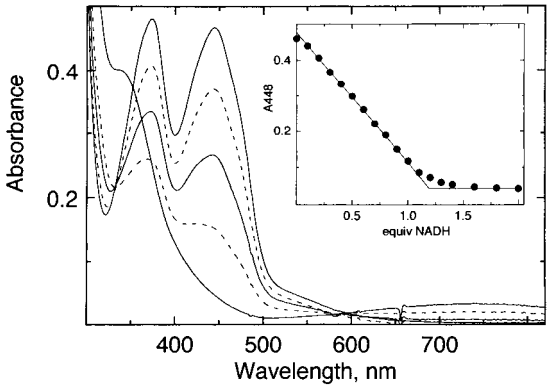

FIGURE 3: Anaerobic titration of the wild-type Nox E/EH_2 form with NADH at pH 8.7. Enzyme (1.0 mL, 39 μM) was reduced in 0.1 M CHES, pH 8.7, containing 1 mM EDTA and 2 mM DTT at 25 °C. Spectra shown in order of decreasing A448 correspond to the starting E/EH_2 form (—) and enzyme after addition of 0.3 (- - -), 0.6 (—), 0.9 (- - -), and 1.6 (—) equiv of NADH/FAD. Inset: Absorbance change at 448 nm versus added NADH. The end point after correction for the slight lag corresponds to 1.1 equiv of NADH/FAD.

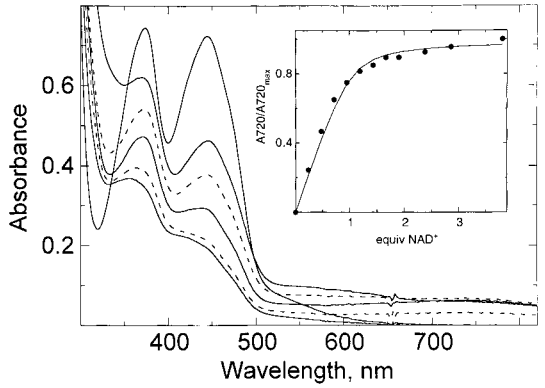

FIGURE 4: NAD^+ titration of the wild-type Nox EH_2'/EH_4 form at pH 8.7. An enzyme solution (1.0 mL) containing 61 μM Nox (E/EH_2) in the pH 8.7 CHES/EDTA/DTT buffer was reduced with 1.0 equiv of NADPH/FAD. The titration data shown were collected after the NADPH syringe was exchanged for one containing anaerobic NAD^+; spectra represent the starting E/EH_2 form (—) and, in order of increasing A448, EH_2'/EH_4 (—) and enzyme after addition of 0.48 (- - -), 1.91 (—), 9.54 (- - -), and 60.2 (—) equiv of $NAD^+/FADH_2$ (the last addition was accomplished by tipping 10 μL of 0.2 M NAD^+ from the cuvette side arm). Inset: Absorbance change at 720 nm versus added NAD^+.

of wild-type Nox involves the FAD/$FADH_2$ potential(s) within the E/EH_2 ⇌ EH_2'/EH_4 redox system. The E/EH_2 form was titrated with dithionite at pH 7.0 in the presence of 2 mM DTT, using 1-deazariboflavin ($E'^0 = -280$ mV; ref *16*) as the reference dye and methyl viologen as the redox communicator. In this manner a value for $E'^0 = -285$ mV was determined for the two flavins of the dimeric wild-type oxidase; there is no indication within experimental limits for any nonequivalence. The 36 mV slope compares favorably with the theoretical value of 29.6 mV for a two-electron transfer at 25 °C (*21*). The titration with NADPH (Figure 1) shows that both FAD on each Nox monomer are essentially fully reduced on addition of 3.26 equiv of NADPH, and 1.56 equiv of $NADP^+$ are formed in the process. From the Nernst equation (*21*) a value for $E_h = -321$ mV can be calculated at this point, consistent with the nearly complete reduction of Nox observed.

Asymmetric Redox Behavior of Reduced Wild-Type Nox at pH 8.7. The midpoint potentials for NADH and NADPH decrease by 30 mV per pH unit at 30 °C (*21*); while the absorbance spectrum of dithionite-reduced recombinant Nox at pH 7.0 ($\lambda_{max} = 357$ nm) is consistent with stabilization of the N(1) anionic form of the dihydroflavin (*1*), the E_m versus pH profile for Nox was not investigated. In preliminary studies in 0.1 M CHES, pH 8.7, we observed that 2 mM DTT quickly reduces the fully oxidized enzyme to the E/EH_2 form; while E_m for DTT does decrease from −332 mV at pH 7.0 to −366 mV at pH 8.1 (*22*), the first pK_a for DTT is 8.3 (*23*). We conclude that the increased concentration of DTT thiolate at pH 8.7 is likely responsible for the enhanced reduction of E → E/EH_2. Therefore, in 0.1 M CHES, pH 8.7, plus 2 mM DTT, titration of wild-type Nox (as the E/EH_2 form due to the presence of DTT) with either NADH or NADPH proceeds to the EH_2'/EH_4 form with a nearly stoichiometric amount of reductant (e.g., 1.1 equiv of NADH per FAD; Figure 3). The active-site asymmetry documented previously is also preserved at the higher pH; the NADPH-reduced enzyme still contains one Cys42-SOH per dimer, as will be demonstrated in the following section. In comparison with Scheme 2, which is derived from titration data at pH 7.0, the behavior of wild-type Nox with NADH at pH 8.7 corresponds directly to the second step of Scheme 2, with DTT replacing the single NADH represented in the first step. With NADPH reduction at pH 8.7 there still is no detectable E−$FADH_2$·$NADP^+$ charge-transfer complex, and with NADH the ϵ720 for the corresponding NAD^+ complex is only 800−900 M^{-1} cm^{-1}, less than half the value at pH 7.0. This observation will be discussed in more detail in the following section.

The observation that NADPH reduction at pH 8.7 is essentially stoichiometric with [E-FAD] also provides the technical basis for titrations of the EH_2'/EH_4 form without complications from redox-linked spectral changes due to NADPH oxidation and/or flavin reduction (e.g., Figure 2). Figure 4 gives the result of an anaerobic NAD^+ titration of the NADPH-reduced EH_2'/EH_4 form at pH 8.7. In the initial phase of this titration, spectral changes are apparent at both 720 nm (E−$FADH_2$·NAD^+) and 448 nm (E−$FADH_2$ → E-FAD), although the A720 change is much more pronounced; while almost 50% of the increase in A720 is attained at 0.5 equiv of NAD^+, only 7% of the total ΔA448 is observed at this point. The direct plot of ΔA720 versus equivalents of NAD^+ with Figure 4 allows the determination of an apparent $K_d = 3.6$ μM for the E−$FADH_2$·NAD^+ complex; this value is similar to that determined at pH 7.0 (5.4 μM; Figure 2). Therefore, the decreased ϵ720 for the complex at pH 8.7 is not due to any increase in $K_d(NAD^+)$ at that charge-transfer $FADH_2$ site. The binding stoichiometry derived from the ΔA720 versus equivalents of NAD^+ plot at pH 8.7 is 1 NAD^+ per $FADH_2$. Difference spectra indicate that the maximal ΔA720 corresponds to the addition of 4−5 equiv of NAD^+; this value then decreases by about 13%, as the titration continues to completion (60 equiv of NAD^+), and an isosbestic point for this second phase appears at about 656 nm. Analysis of the absorbance change at 448 nm indicates that on completion of the full titration 52% (one $FADH_2$ per dimer) of the reduced flavin complement has been oxidized, and a direct plot of the A448 data set versus equivalents of NAD^+ gives an apparent K_d of 0.14 mM.

Scheme 4

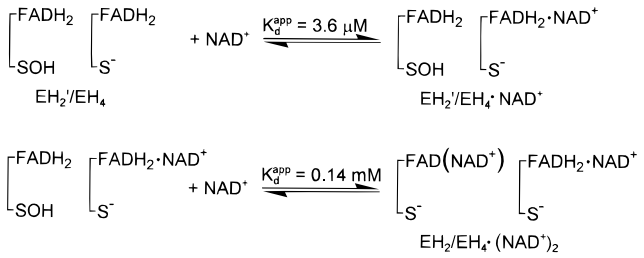

An interpretation of the qualitative observations presented would suggest that the two $FADH_2$ per dimer behave differently as NAD^+ is added; at relatively low [NAD^+] the process of a simple binding interaction with $FADH_2$ at one site, giving rise to the $FADH_2 \rightarrow NAD^+$ charge-transfer band centered at 720 nm, predominates. This process also corresponds to an increase in absorbance at 377 nm which may reflect further stabilization of the N(1) anionic form of $E-FADH_2$. As the A720 increase comes to completion, the second phase, which consists of reoxidation of one $FADH_2$ per dimer as evidenced over the wavelength range 330−500 nm, begins to predominate. Associated with this $FADH_2$ oxidation is an increase at long wavelength between 500 and 650 nm which is attributed to the EH_2 charge-transfer band that develops as the result of intramolecular electron transfer within the EH_2' subunit. The binding of NAD^+ in this phase (apparent $K_d = 0.14$ mM) leads to reduction of the EH_2' Cys42-SOH at the expense of $FADH_2$; it is equally clear that oxidation of this $FADH_2$ has only a small effect on ϵ720 for the $EH_4 \cdot NAD^+$ complex, further supporting the conclusion that the two active sites per dimer interact independently with NAD^+. These interpretations are summarized in Scheme 4. The ΔA720 titration data (Figure 4) are clearly consistent with binding of one NAD^+ per $FADH_2$; in addition, the difference spectra (not shown) through 0.2 mM NAD^+ indicate only a small increase in A340, suggesting that little if any NAD^+ reduction is occurring. Throughout the titration the increase in A530 due to nascent EH_2 thiolate closely parallels the ΔA448, supporting the conclusion that intramolecular electron transfer to Cys42-SOH, not reduction of NAD^+, accounts for the measured $FADH_2$ oxidation.

In comparing this titration result with that at pH 7.0, the oxidation of one $FADH_2$ per dimer is consistent with the oxidation of 0.58 mol of NADPH per subunit in the linear phase of the pH 7.0 experiment. One indication of differences in behavior at the two pH values, however, concerns the ϵ720 value for the fully reduced $E-FADH_2 \cdot NAD^+$ complex at pH 7.0 (1920−2360 M^{-1} cm^{-1}) and the values at pH 8.7 for both the NADH-reduced (Figure 3) and NAD^+-titrated (Figure 4) enzyme forms (900−1100 M^{-1} cm^{-1}). The observation that the final species resulting at pH 8.7 from NADH titration (100% E-$FADH_2$) and from NAD^+ titration of EH_2'/EH_4 (50% $E-FADH_2$) give the same ϵ720 value also suggests that only one $FADH_2$ per dimer in the former case is involved in the observed charge-transfer interaction with NAD^+.

Interactions of Reduced Wild-Type Nox with AcPyAD$^+$ and AAD$^+$. The preceding section demonstrates that at pH 8.7 NAD^+ titration of the Nox EH_2'/EH_4 species induces quite different responses in each of the two active sites per dimer, but little if any net electron transfer from reduced Nox to

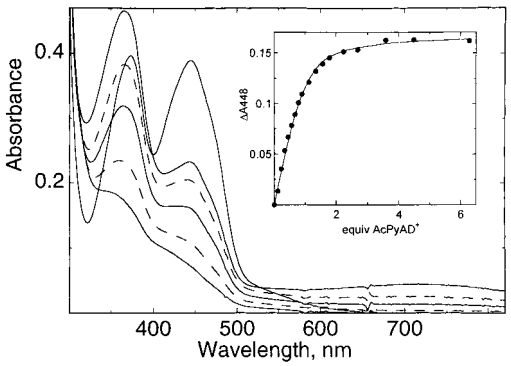

FIGURE 5: $AcPyAD^+$ titration of the wild-type Nox EH_2'/EH_4 form at pH 8.7. A 33 μM E/EH_2 solution was reduced with 1.1 equiv of NADPH/FAD, as described in Figure 4. Spectra shown represent the starting E/EH_2 form (—) and, in order of increasing A448, EH_2'/EH_4 (—) and enzyme after addition of 0.22 (- - -), 0.67 (—), 1.35 (- - -), and 6.28 (—) equiv of $AcPyAD^+/FADH_2$. Inset: Absorbance change at 448 nm versus added $AcPyAD^+$.

NAD^+ is observed. We further examined the possible connection between the pyridine nucleotide redox potential and the interaction with reduced Nox by titrating the enzyme with $AcPyAD^+$ and AAD^+, respectively. E'^0 for the AcPyADH/$AcPyAD^+$ couple is −248 mV, or 72 mV more positive than NADH/NAD^+ (*24*). AAD^+ is a nonreducible analogue of NAD^+ (*25*) whose intrinsic fluorescence and absorbance properties allow more direct spectral analyses of enzyme binding. As shown in Figure 5, titration of EH_2'/EH_4 with $AcPyAD^+$ results in a very different pattern of binding and redox behavior. In contrast to the NAD^+ titration, the increase in A448 precedes the formation of the charge-transfer complex at 720 nm, with respect to equivalents of $AcPyAD^+$ added. The midpoint of the A448 increase corresponds to an [$AcPyAD^+$] where only 29% of the total ΔA720 is observed; with NAD^+ the stable $E-FADH_2 \cdot NAD^+$ complex was fully formed before the midpoint was reached at 448 nm.

In conjunction with the $E-FADH_2$ oxidation, which reaches a maximum of 52% (one $FADH_2$ per dimer) at saturating (0.21 mM) $AcPyAD^+$, the large increase in A368 is due to the reduction of $AcPyAD^+ \rightarrow$ AcPyADH ($\lambda_{max} =$ 363 nm, $\epsilon 363 = 9100$ M^{-1} cm^{-1}; ref *26*), again in contrast to the behavior with NAD^+. Fluorescence quantitation (corrected for the contribution from E−FAD) indicates that a minimum of 0.38 mol of AcPyADH per flavin (0.76 equiv per enzyme dimer) is formed; the $FADH_2$ oxidation observed is largely if not entirely coupled to $AcPyAD^+$ reduction, and not to intramolecular Cys42-SOH reduction. This behavior is generally consistent with the +72 mV separation in E_m values for $AcPyAD^+$and NAD^+ at pH 7.0, and this difference should also apply at pH 8.7 provided ΔE_m/pH for AcPyADH/$AcPyAD^+$ is about −30 mV. From the direct plot of ΔA448 versus equivalents of $AcPyAD^+$ we can determine that the oxidation of $E-FADH_2$ corresponds to a stoichiometry of one $AcPyAD^+$ per flavin. After correcting the total [$AcPyAD^+$] added for the formation of AcPyADH, a similar plot of ΔA720 gives an apparent K_d of 5.8 μM with a similar unit stoichiometry. Under nearly identical conditions the apparent K_d value for NAD^+ at the charge-transfer $E-FADH_2$ site is 3.6 μM. In addition, the ϵ720 value for the stable $E-FADH_2 \cdot AcPyAD^+$ complex at pH 8.7 (1330 M^{-1} cm^{-1}) is significantly lower than that obtained by AcPyADH

Scheme 5

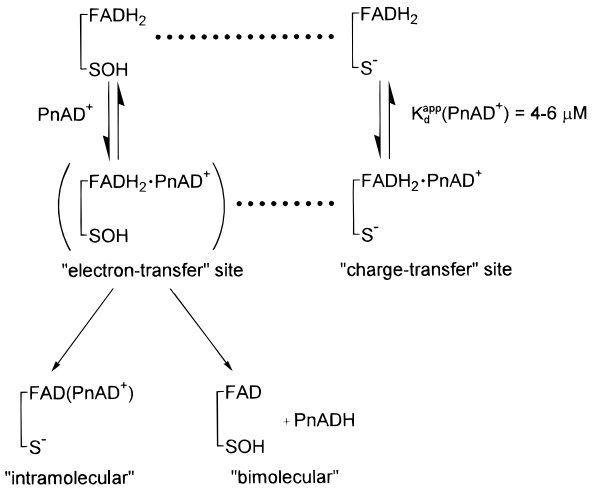

reduction of Nox at pH 7.0 (4220 M^{-1} cm^{-1}), consistent with the spectral properties of the NAD^+ complex at pH 8.7 and 7.0, respectively. The NAD^+ and $AcPyAD^+$ titrations are alike in that only one $FADH_2$ per Nox dimer is reoxidized. Furthermore, it is tempting to speculate that the EH_2' subunit that undergoes intramolecular oxidation−reduction promoted by NAD^+ binding is also responsible for the E−$FADH_2$ oxidation coupled to $AcPyAD^+$ reduction. In each case the charge-transfer $FADH_2$ site binds the respective pyridine nucleotide (with very similar apparent K_d values), leading to the stable complex which is not involved in redox activity beyond the charge-transfer interaction. As shown in Scheme 5, the remaining $FADH_2$ site ultimately participates in electron transfer as promoted by pyridine nucleotide binding. With the lower E_m of NADH/NAD^+ the intramolecular path of electron transfer is favored (Cys42-SOH reduction), but with $AcPyAD^+$ the bimolecular path leading to AcPyADH formation is preferred. The charge-transfer $FADH_2$ sites of any of these enzyme forms can also be occupied through linked equilibria with NAD^+ or $AcPyAD^+$, but the two types of interactions at the two active sites per dimer appear to be independent.

When the reduced enzyme was titrated at pH 8.7 with AAD^+, we expected to see intramolecular Cys42-SOH reduction since bimolecular electron transfer to AAD^+ is not possible. In this experiment, however, addition of 11 equiv of AAD^+ per flavin (final [AAD^+] = 0.34 mM) led to only a very small increase (about 0.025) in A448. While the AAD^+ titration also failed to give any increase in A720 indicative of a developing charge-transfer interaction, this observation can be attributed to the unusual redox properties of AAD^+ (*25*). Since other observations cited previously indicate that pyridine nucleotide binding may be affected at pH 8.7, fluorescence analysis of AAD^+ (λ_{max}^{ex} = 331 nm, λ_{max}^{em} = 420 nm; ref *25*) binding to reduced Nox was also performed; this result shows clearly that addition of up to 2.1 equiv per $FADH_2$ does not correspond to any fluorescence quenching. To test the suggestion that poor AAD^+ binding was a result of the higher pH, the titration was repeated at pH 7.0 with dithionite-reduced Nox, since AAD^+ does not form a sulfite adduct like NAD^+ or $AcPyAD^+$. In this case (data not shown) 44% of the total E−$FADH_2$ is oxidized (0.88 FAD formed per dimer) on addition of 5.2 equiv of AAD^+. Again, since the redox properties of AAD^+ preclude any charge-transfer with E−$FADH_2$ (*25, 27*), difference spectra clearly show the nascent EH_2 charge-transfer band centered at about 520 nm, which develops as the EH_2' subunit is converted to EH_2 on AAD^+ binding. The pH 8.7 results in summary indicate that the electron-transfer $FADH_2$ site (EH_2' subunit) is very sensitive to pH as well as to the nature of the substituent at the 3-position of the pyridinium ring. With $AcPyAD^+$ 50% of the total $FADH_2$ oxidation observed is seen with 0.6 equiv per flavin, with NAD^+ the apparent K_d is 0.14 mM, and AAD^+ does not bind.

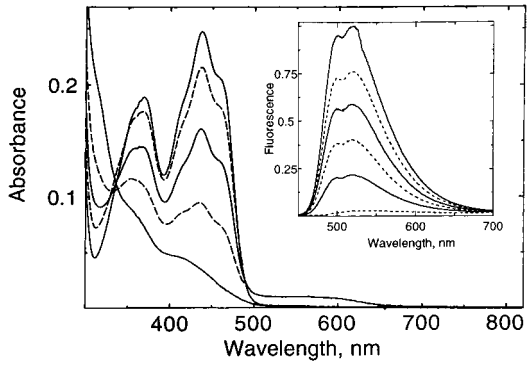

FIGURE 6: Dithionite titration of C42S Nox at pH 7.0. Enzyme (0.7 mL, 18.8 μM) was reduced in 50 mM phosphate, pH 7.0, containing 0.5 mM EDTA plus 2 mM DTT. Spectra shown in order of decreasing A438 correspond to oxidized enzyme (—) and enzyme after addition of 0.21 (- - -), 0.52 (—), 0.86 (- - -), and 1.90 (—) equiv of dithionite/FAD. The end point at 438 nm corresponds to 1.1 equiv of reductant/FAD. Inset: Dithionite titration of C42S Nox in a similar experiment monitoring enzyme fluorescence (λ^{ex} = 438 nm); [enzyme] was 35.2 μM, and DTT was absent.

Redox Properties of C42S Nox. We have recently shown (*9*) that NADH titration of C42S Nox in 50 mM phosphate, pH 7.0, plus 0.5 mM EDTA leads to direct flavin reduction with 1 equiv of NADH. Figure 6 presents a similar experiment in which the mutant enzyme is titrated with dithionite; full reduction requires 1.1 equiv per FAD, again confirming that replacement of Cys42 with Ser eliminates the non-flavin redox center. In addition, a small amount of neutral blue semiquinone, which is not seen during dithionite reduction of wild-type Nox, appears during the course of reduction. Using ϵ610 = 3900−4150 M^{-1} cm^{-1} as determined for the neutral semiquinones of flavodoxin and glucose oxidase (*28, 29*), we can estimate that the radical form of C42S Nox accounts for about 15% of the total enzyme at maximal formation. This is similar to the extent of blue semiquinone stabilization seen on reduction of wild-type Nox in the presence of azide (*14*). It appears from the near-UV spectrum of reduced C42S Nox that the N(1) anionic form of $FADH_2$ is stabilized at pH 7.0 (*30*). As stated recently (*9*), the fluorescence yield of the mutant enzyme is 37% that of free FAD, or twice that of fully oxidized wild-type Nox. Unlike free FAD or wild-type enzyme, however, the emission spectrum of the C42S mutant exhibits a striking shoulder at 500 nm in addition to λ_{max}^{em} = 520 nm (Figure 6). The excitation spectrum (λ^{em} = 520 nm) is not distinguishable from the C42S absorbance spectrum, and both features in the emission spectrum are reduced together on titration with dithionite.

In a separate experiment the redox potential for the FAD/$FADH_2$ couple in the C42S mutant was determined at pH

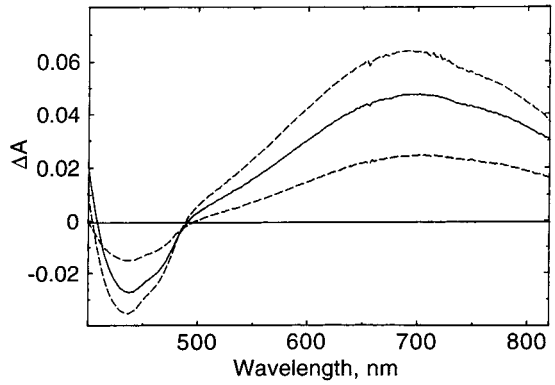

FIGURE 7: Temperature dependence of the reduced C42S Nox·AcPyAD$^+$ charge-transfer spectrum. Difference spectra (minus the spectrum recorded at 45 °C) in order of increasing A700 represent the E−FADH$_2$·AcPyAD$^+$ complex (38.6 μM) at 35 °C (- - -), 25 °C (—), and 10 °C (- - -). All changes were fully reversible, and in each case the sample was allowed to reach equilibrium at the new temperature before the final spectrum was recorded. The complex was prepared in the phosphate/EDTA buffer, pH 7.0, by reducing the enzyme with 3.93 equiv of AcPyADH/FAD.

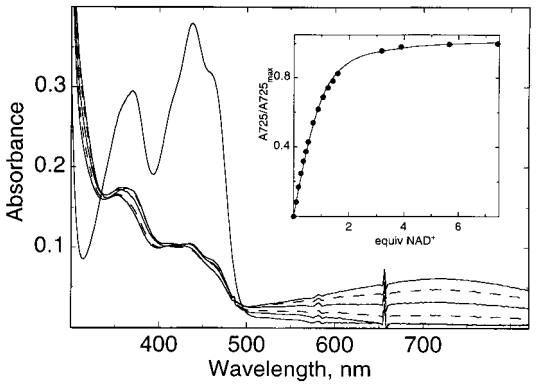

FIGURE 8: NAD$^+$ titration of reduced C42S Nox at pH 7.0. Enzyme (1.0 mL, 28 μM) was reduced with 1.1 equiv of NADPH/FAD in the phosphate/EDTA buffer. The titration data shown were collected after the NADPH syringe was exchanged for one containing 1.4 mM NAD$^+$; spectra represent the starting oxidized (—) and reduced (—) enzymes and, in order of increasing A725, the reduced enzyme after addition of 0.18 (- - -), 0.53 (—), 1.06 (- - -), and 7.43 (—) equiv of NAD$^+$/FADH$_2$. Inset: Absorbance change at 725 nm versus added NAD$^+$.

7.0, following the identical protocol (except for the absence of DTT) as described for wild-type Nox. $E'^0 = -275$ mV (data not shown), only 10 mV more positive than that for the wild-type E/EH$_2$ form, and the corresponding slope is 33 mV. This result contrasts sharply with that observed on replacement of Cys42 with Ser in the closely related NADH peroxidase (Npx; ref *11*); in that case the flavin potential increases by 93 mV in the mutant and reflects the strong influence of Cys42-S$^-$ (and the Npx EH$_2$ charge-transfer interaction) on the redox properties of the flavin. The Nox mutant can still be reduced (pH 7.0) in the presence of an excess of AcPyADH, where the redox potentials are separated by only 27 mV. As with wild-type Nox a very similar E−FADH$_2$·AcPyAD$^+$ complex results, and ϵ720 for the AcPyAD$^+$ complex (3380 M^{-1} cm^{-1}) is almost double that for the reduced C42S·NAD$^+$ complex (1860 M^{-1} cm^{-1}) at 25 °C. Furthermore, the absorbance spectra for both charge-transfer complexes show a dramatic dependence on temperature over the range 10−45 °C, which is fully reversible (Figure 7). Similar behavior was documented previously for the NAD$^+$ complex of the reduced form of inactive wild-type Nox (*2*).

Replacement of Cys42 Eliminates the Intramolecular Path for NAD$^+$-Induced Electron Transfer. We have proposed that the active-site asymmetry observed in NAD(H) titrations of reduced and oxidized forms of wild-type Nox is directly attributable to the nonequivalence of the two Cys42-SOH centers per dimer (*2*); a rather direct prediction based on this model is that NAD$^+$ titration of reduced C42S Nox should not give rise to flavin reoxidation. Since the E'^0 value for the mutant enzyme is higher than that for wild-type enzyme, we were able to obtain essentially full reduction with stoichiometric NADPH at pH 7.0. As shown in Figure 8, there is a small amount of residual semiquinone in the reduced enzyme preparation. As NAD$^+$ is added anaerobically, the charge-transfer absorbance of E−FADH$_2$·NAD$^+$ develops immediately, but there is no hint of flavin oxidation even as [NAD$^+$] reaches 0.21 mM at the end of the titration. The difference spectra also indicate that NAD$^+$ reduction does not occur, and there are perturbations of the reduced flavin spectrum that are consistent with increased N(1) anionic character (ΔA_{max} at 376 nm) and resolution in the 465 nm range. The K_d determined by a direct plot of ΔA725 versus equivalents of NAD$^+$ is 3.9 μM, and the binding stoichiometry is 1.1 NAD$^+$ per FADH$_2$. This K_d can be compared to the apparent K_d values of 5.4 μM and 3.6 μM as obtained with NAD$^+$ for the charge-transfer site in reduced wild-type Nox at pH 7.0 and 8.7, respectively. The ϵ725 value for the mutant complex at saturating [NAD$^+$] is 2150 M^{-1} cm^{-1}; this compares favorably with the ϵ725 of 1860 M^{-1} cm^{-1} which results on NADH titration of the mutant at pH 7.0, 25 °C (*9*). This experiment conclusively demonstrates that the Cys42-SOH center in wild-type Nox is the electron acceptor within the EH$_2'$/EH$_4$ form that is responsible for E−FADH$_2$ oxidation (one per dimer) on NAD$^+$ binding.

Titrations of Reduced C42S Nox with AcPyAD$^+$ and AAD$^+$. The results with wild-type Nox indicate that pyridine nucleotide binding to the "electron-transfer" FADH$_2$ site leads to reduction of either Cys42-SOH or the pyridine nucleotide, depending primarily on the redox potential of the latter. Mutagenesis of Cys42 should eliminate the former possibility, as demonstrated in the preceding experiment, but should have no obvious effect on the reduction of AcPyAD$^+$, for example. To test this, the reduced mutant was titrated with AcPyAD$^+$ under anaerobic conditions. As shown in Figure 9, there are changes in absorbance indicative of both E−FADH$_2$·AcPyAD$^+$ complex formation (ΔA700) and a modest extent of enzyme reoxidation (ΔA438 equivalent to 21% of total E−FADH$_2$). A direct plot of the A700 data gives a stoichiometry of 1.1 AcPyAD$^+$ per subunit. The difference spectra also show, as was the case with wild-type Nox, that the extent of E−FADH$_2$ oxidation is accounted for quantitatively by the formation of AcPyADH (ΔA_{max} = 370 nm and fluorescence). A final demonstration of the altered redox behavior of C42S Nox involved AAD$^+$ titration of dithionite-reduced mutant enzyme at pH 7.0; under identical conditions titration of reduced wild-type Nox gives 44% flavin reoxidation. While there are small changes in reduced C42S absorbance in the 400−600 nm range which are consistent with perturbations in the E−FADH$_2$ spectrum, there is no flavin reoxidation.

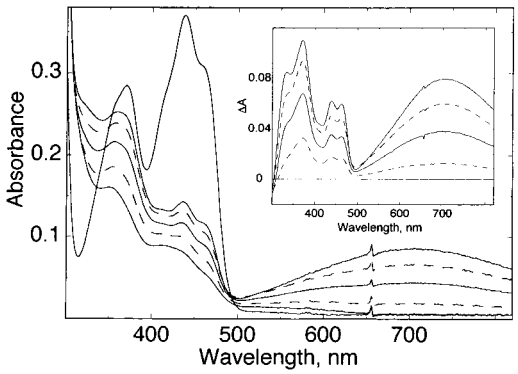

FIGURE 9: AcPyAD$^+$ titration of reduced C42S Nox at pH 7.0. Enzyme (1.0 mL, 27 μM) was reduced with 1.1 equiv of NADPH/FAD as described in Figure 9. Spectra shown represent the starting oxidized (—) and reduced (—) enzymes and, in order of increasing A700, the reduced enzyme after addition of 0.21 (- - -), 0.53 (—), 0.95 (- - -), and 5.04 (—) equiv of AcPyAD$^+$/FADH$_2$. Inset: Difference spectra (minus free reduced enzyme) shown in order of increasing [AcPyAD$^+$].

Scheme 6

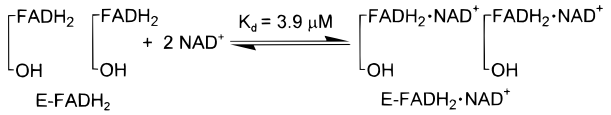

Scheme 7

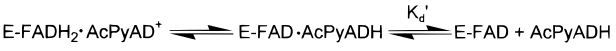

Mutagenesis of the Cys42-SOH redox center in Nox certainly eliminates the intramolecular path for electron transfer from FADH$_2$, and there is no evidence from the static titrations presented with NAD$^+$ (or NADH) that C42S Nox retains any element of the intrinsic asymmetry indicated for the wild-type enzyme in Scheme 5. At pH 7.0 both FADH$_2$ on each monomer behave identically in terms of the affinity and stoichiometry of NAD$^+$ binding (see Scheme 6). While AcPyAD$^+$ titration of the reduced mutant does yield partial FADH$_2$ oxidation along with stable E−FADH$_2$·AcPyAD$^+$ complex formation, the stoichiometry of the electron-transfer component is very different from that seen with wild-type Nox and does not directly support the model (Scheme 5) for independent, nonequivalent flavin sites in the dimer. Rather the AcPyAD$^+$ results with C42S Nox can be accommodated by a simple extension adapted from Scheme 6 (see Scheme 7). As shown in Scheme 7 the extent of FADH$_2$ oxidation observed is a function of the two K_d values as well as the redox potentials for flavin and pyridine nucleotide.

DISCUSSION

The existence of asymmetry within pyridine nucleotide-complexed dimers has previously been demonstrated under equilibrium conditions for pig heart lipoamide dehydrogenase (LipDH; refs *27* and *31*) and for the mercuric reductase (MR; ref *10*) encoded by *Pseudomonas* transposon Tn501. Thorpe and Williams (*27*) showed that addition of NAD$^+$ to the monoalkylated EHR form of LipDH over the pH range 6.0−8.8 led to partial (0.8−1 FAD per dimer) formation of an FAD C(4a)-adduct with the charge-transfer Cys50 thiol; at pH 7.6 and 8.8 (15 °C) only 1.1−1.2 NAD$^+$ were bound per enzyme dimer. The flavin fluorescence of EHR was quenched by 50% as well, supporting the conclusion that NAD$^+$ binding and C(4a) adduct formation involved one active site per dimer. Quite different behavior was observed with the NAD$^+$ analogues AAD$^+$ and AcPyAD$^+$; at pH 7.6 two AAD$^+$ were bound per EHR dimer, restoring the Cys50-S$^-$ → FAD charge-transfer band centered at 580 nm, which is disrupted on alkylation, but no detectable C(4a) adduct formation resulted.

While mercuric reductase is also a member of the pyridine nucleotide-disulfide oxidoreductase family (*32*) and shares many properties with LipDH and glutathione reductase (GR), this enzyme is unique in that two pairs of Cys residues are found within the active site (*33*). Cys135 and Cys140 constitute the redox-active disulfide which is formally equivalent to those found in LipDH and GR. While both Cys557′ and Cys558′ (formerly referred to as Cys558′ and Cys559′; see ref *34*) are required for optimal reduction of Hg(SR)$_2$, neither is essential as a ligand in the reducible Hg(II) enzyme complex. Recent evidence (*34*) indicates that these C-terminal cysteines, in particular Cys557′, are required to mediate access of Hg(SR)$_2$ to the redox-active Cys135, Cys140 pair. The crystal structure of MR (*35*) shows that the redox-active disulfide and the C-terminal cysteines within a given active site are derived from the two respective subunits within the homodimer. A third pair of N-terminal cysteines (Cys10, Cys13) is not essential for efficient reduction of Hg(II) (*10*). Miller et al. (*10*) have described a number of lines of evidence supporting subunit asymmetry in both wild-type and mutant forms of MR. One group of equilibrium analyses indicating half-sites asymmetry included titration of the C135A/C557A/C558A mutant with AADP$^+$, where 50% formation (one FAD per dimer) of the FAD C(4a) thiol adduct with Cys140 was observed on addition of two AADP$^+$ per dimer (K_d^{app} = 0.2 μM). In addition, NADPH titrations of the C10A/C13A mutant (pH 5.1) and C135A/C140A mutant (pH 7.3) both led to reduction of only one FAD per dimer. A second group of equilibrium analyses, for direct ligand-binding processes without associated redox chemistry, included titration of the wild-type EH$_2$ form with NADP$^+$, where absorbance changes at 350 and 430 nm corresponded to stoichiometries of 0.5 and 1 equiv of NADP$^+$ per FAD, respectively. NADPH titrations of EH$_2$ (pH 7.3) and the C135A mutant (pH 8.5) led to either differential behavior in which the titration data at different wavelengths corresponded to different stoichiometries or biphasic behavior at the indicated wavelengths. Combined with the differential kinetic behavior observed in the oxygen reaction of the NADPH-complexed C135A/C140A mutant, these results were interpreted in support of an alternating sites mechanism for catalysis with the dimeric enzyme. The alternating sites mechanism proposed for MR (*10*) involves simultaneous "binding" and "catalytic" events on the two subunits of the dimer; completion of one coordinated set of events leads to coupled conformational change(s) which invert(s) the roles of the two subunits. An important advantage to the resulting catalytic mechanism is the coupling of energetically favorable and unfavorable reactions, both within and between the two active sites per dimer; subunit communication is essential for mediating those changes across the dimer interface.

Like LipDH and MR, Nox and its closely related homologues Npx (*6*) and coenzyme A-disulfide reductase (*36*) are members of the glutathione reductase class of NAD(P)H-dependent flavoprotein disulfide reductases (*32*). The utilization of the Cys-SOH redox center instead of a redox-active disulfide represents the primary point of contrast between Nox and Npx (peroxide reductases) and the true disulfide reductases. In this work we have shown that, as expected, reduction of the C42S Nox mutant lacking the non-flavin redox center requires 1.1 equiv of dithionite per FAD; we have previously demonstrated the same unit stoichiometry with NADH as reductant (*9*). The most significant difference in the spectral courses of the two titrations at pH 7.0 is the appearance of the $FADH_2 \rightarrow NAD^+$ charge-transfer band centered at about 725 nm ($\epsilon 725 = 1860\ M^{-1}\ cm^{-1}$ at 25 °C). Titration of reduced C42S Nox at pH 7.0 with NAD^+ gives a K_d value of 3.9 μM for this interaction (Scheme 6) with a similar $\epsilon 725$ value of 2150 $M^{-1}\ cm^{-1}$. The qualitative behavior observed for reduced C42S Nox in these static titrations with NAD^+ and $AcPyAD^+$ is in fact quite similar to that described for the reduced melilotate hydroxylase·substrate complex (*37*). Kinetic analysis of the reaction with $AcPyAD^+$ under pseudo-first-order conditions, for example, clearly showed the initial formation of the $E-FADH_2$·$AcPyAD^+$·S charge-transfer complex, followed by the slower electron-transfer step leading to the final equilibrium concentrations of charge-transfer complex and oxidized enzyme (plus AcPyADH and free $AcPyAD^+$).

Reduced C42S Nox complexes with NAD^+ and $AcPyAD^+$ show striking inverse dependencies on temperature (10−45 °C), with regard to the intensity of the respective charge-transfer band. This effect, which leads to a reduction in $\epsilon 700$ of 45% for the $AcPyAD^+$ complex over the indicated range, is not attributable to changes in K_d for binding of the pyridine nucleotide and is also fully reversible. We have previously shown (*14*) in a study of Nox as reconstituted with a series of FAD analogues (free solution E'^0 values ranging from −55 to −335 mV) that the reduced enzyme·NAD^+ complexes do not show a strong correlation for either λ_{max} or intensity with the expected change in charge-transfer donor strength. Massey and Palmer (*38*), in contrast, did observe the expected red shift in λ_{max} for the charge-transfer complexes of reduced LipDH with NAD^+ and thionicotinamide adenine dinucleotide, respectively, where E'^0 for the acceptor increases by 35 mV. With $AcPyAD^+$, however, direct reoxidation of $E-FADH_2$ was observed; as in the present study $NADP^+$ failed to give complex formation. The reduced LipDH·NAD^+ complex also exhibited a temperature dependence (4−38 °C) for $\epsilon 700$ qualitatively similar to that seen with C42S Nox, although the extent of $\Delta\epsilon 700$ was much smaller than that observed in the present study. In comparing the properties of these charge-transfer complexes of Nox and LipDH, it should also be pointed out that the $FAD/FADH_2$ potential for LipDH is 71 mV more negative (*39*) than that for C42S Nox at pH 7.0.

The characterization of C42S Nox in the present study demonstrates that Cys42, almost certainly in the Cys42-SOH/Cys42-SH form as proposed, is the non-flavin redox center in the wild-type enzyme. The behavior of reduced C42S Nox toward NAD^+ also confirms that it is this Cys42-SOH center that is the basis for the asymmetric redox behavior observed with wild-type enzyme, leading to the requirement of only 1.5−1.6 equiv of dithionite or NADPH per FAD in forming the mixed EH_2'/EH_4 dimer (Scheme 2). The remaining oxidized Cys42-SOH center also serves as the intramolecular electron acceptor when NADPH-reduced Nox is titrated with NAD^+ at pH 7.0 or 8.7; in the latter case oxidation of one FAD per dimer is observed directly (Scheme 4). At pH 7.0 the nascent oxidized FAD is readily reduced by the excess NADPH already present, leading to oxidation of 1.16 equiv of NADPH per dimer in the linear phase of the NAD^+ titration (Scheme 3). Enzyme-monitored turnover analysis of the wild-type Nox reaction (as with the C42S Nox reaction; ref *40*) is consistent with the participation of a reduced enzyme·NAD^+ complex in the catalytic cycle, since a largely reduced species with long-wavelength absorbance ($\lambda_{max} = 715$ nm at 5 °C) predominates in the diode-array spectrum at steady state. While a detailed description of this and other observations on the kinetic mechanism will be provided in a separate communication,[2] it is also clear that at steady state wild-type Nox is catalyzing the fully coupled reduction of $O_2 \rightarrow 2H_2O$ (*14*), without detectable H_2O_2 or superoxide production. The combination of static and kinetic results at pH 7.0 suggests either that reduction of Nox with excess NADH yields the dimeric EH_4·NAD^+ form directly [in contrast to the EH_2'/EH_4·$(NAD^+)_2$ form observed in static titrations] or that the asymmetric EH_2'/EH_4·$(NAD^+)_2$ species is the true catalytic intermediate in the wild-type Nox reaction; during turnover a conformational or chemical change leads to reduction of the EH_2' subunit ($EH_2' \rightarrow EH_4$·NAD^+) prior to its reaction with oxygen. Such an alternating sites mechanism would also be consistent with that summarized for C42S Nox (see Scheme 8).

The indication of nonequivalent NAD^+-binding sites for wild-type Nox at pH 7.0 (Figure 2) is fully supported by three key observations at pH 8.7. Direct NADH titration at the higher pH yields an $E-FADH_2$·NAD^+ complex with $\epsilon 720$ (800−900 $M^{-1}\ cm^{-1}$) less than half that obtained (2360 $M^{-1}\ cm^{-1}$) in a similar titration at pH 7.0. When NADPH-reduced Nox is mixed directly with 2 mM NAD^+, an initial complex with $\epsilon 720 = 900\ M^{-1}\ cm^{-1}$ appears (data not shown); over time, however, this is converted to a stable complex with $\epsilon 720 = 1760\ M^{-1}\ cm^{-1}$, an increase of almost exactly 2-fold. Furthermore, the NAD^+ titration at pH 8.7 demonstrates clearly that the charge-transfer site saturated at low [NAD^+] ($K_d^{app} = 3.6$ μM) is independent from the NAD^+-binding site that gives rise to $FADH_2$ oxidation; as one $FADH_2$ per dimer is oxidized, there is only a small perturbation in A720. The $FADH_2$ at this electron-transfer site is distinct from that required for the charge-transfer interaction (Scheme 5). The same distinction appears on titration with $AcPyAD^+$, except there is a qualitative difference in the nature of the observed electron-transfer component. The concept of charge-transfer and electron-transfer $FADH_2$ sites in wild-type Nox, based on these equilibrium analyses, is also relevant to the kinetic inequivalence reported recently (*9*) for the oxidative half-reaction of reduced C42S Nox·NAD^+. The fully reduced $E-FADH_2$·NAD^+ dimer reacts with O_2 ($k = 8.5 \times 10^5\ M^{-1}\ s^{-1}$ at 5 °C) at one $FADH_2$ only, yielding the mixed $E-FADHOOH(NAD^+)/E-FADH_2$·$NAD^+$ dimer which has been characterized by spectral and kinetic analyses (see also Scheme 1). In keeping with the

[2] T. C. Mallett and A. Claiborne, unpublished results.

Scheme 8

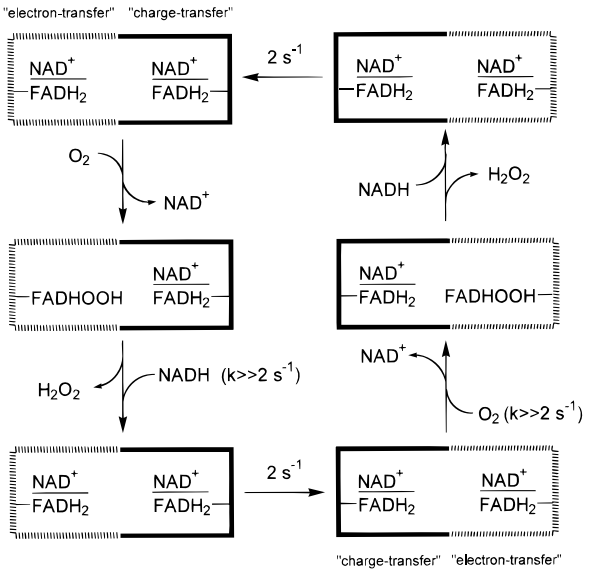

electron-transfer versus charge-transfer functions described above, FAD C(4a)-hydroperoxide formation involves two-electron reduction of O_2; the second $FADH_2$ maintains its charge-transfer status (see Scheme 8).

Only after the peroxyflavin component completes its catalytic cycle, releasing H_2O_2 and NAD^+, does oxygen reactivity at the second $FADH_2$ site proceed. The rate-limiting step in reoxidation has been ascribed to a chemical or conformational change ($k = 2\ s^{-1}$ at 5 °C) which also matches k_{cat}. Although flavoprotein oxidases and monooxygenases generally react rapidly with O_2 (*41*), it has also been recognized for a number of years that the reactivity of $FADH_2$ (or $FMNH_2$) with O_2 is modulated by the protein environment; therefore, rate differences of at least 10^6 are found among flavoproteins. The conformational change described for C42S Nox is likely a form of subunit communication which modulates the environment of the charge-transfer $FADH_2$, converting it effectively to an O_2-reactive (electron-transfer) site within a catalytically competent time frame. While these oxidative half-reaction studies were of necessity conducted in the absence of NADH, it is likely that NADH reduction of the nascent FAD appearing at the primary O_2-reactive site occurs rapidly (i.e., $\gg 2\ s^{-1}$). This energetically favorable process may contribute to the conformational change involved in subunit communication in a manner similar to that proposed by Miller et al. (*10*) for mercuric reductase (inversion of charge-transfer and electron-transfer sites in the case of C42S Nox). Still the limiting rate constant of $2\ s^{-1}$ is observed both in turnover (excess NADH) and in the absence of NADH, so any such contribution would not appear to affect the rate constant for the conformational change per se.

The crystal structures of the Cys42-sulfonic acid derivative of *E. faecalis* Npx (*42*) and its complex with NADH (*43*) suggest two possible structural factors which might contribute to the subunit communication involved in this version of an alternating sites mechanism for catalysis by C42S Nox. In the 2.16 Å structure of the free enzyme there is only one contribution from the second subunit to the active site located on the primary subunit; this consists of an intersubunit hydrogen bond between FAD N(3)−H and Phe424′−O. In addition, the structure of the NADH complex shows that while the aromatic ring of Tyr159 covers the isoalloxazine ring of FAD in the free enzyme, Tyr159 swings out on NADH binding. Both Phe424 and Tyr159 of Npx are conserved in Nox (*12*) and could potentially participate in intersubunit communication of the type described in Scheme 8, modulating the properties of the second active site in response to changes in flavin redox state and/or NAD^+-binding status at the primary active site.

While these kinetic studies of O_2 reactivity apply strictly to C42S Nox, it is clear that at pH 7.0 NADH titration of the wild-type enzyme leaves one Cys42-SOH per dimer. Given the relatively high value of E'^0 indicated for the Cys42-SOH/-SH couple in Npx (*18*), it seems most likely that some conformational rather than chemical barrier is involved in "masking" this redox center, in keeping with the observation that the productive electron-transfer interaction of this Cys42-SOH with $FADH_2$ is induced on NAD^+ binding. At the same time there is a clear functional rationale for blocking O_2 reactivity at the $EH_2'{\cdot}NAD^+$ site, since this would lead directly to the formation of potentially deleterious H_2O_2, not $2H_2O$. The conformational change identified kinetically with C42S Nox, and which may be related to that described in this study, could have the effect of promoting O_2 reactivity at the second $FADH_2$ site in wild-type Nox only after reduction of the associated Cys42-SOH center ($EH_2' \rightarrow EH_4$), thus ensuring the fully coupled reduction of $O_2 \rightarrow 2H_2O$ in steady-state turnover.

Therefore, it is very important to state carefully that while mutagenesis of the Cys42-SOH redox center in Nox eliminates the path for intramolecular electron transfer from $FADH_2$, therefore eliminating the asymmetric binding and redox behavior with pyridine nucleotides as observed with wild-type Nox under equilibrium conditions, the same C42S mutant clearly exhibits kinetic inequivalence in its O_2 reaction mechanism—and the conformational changes and/or subunit communication involved in the two cases may be closely related or identical. It is also important to stress that a similar type of control is observed with the Nox homologue coenzyme A-disulfide reductase, as has been described in a separate communication.[3] Finally, this study adds to our structural understanding of the functional divergence between Nox and the closely related Npx, with a major distinction being facile NADH reduction of $EH_2 \rightarrow EH_4$ only with Nox. E'^0 for the respective $FAD/FADH_2$ couples is increased from −312 mV for Npx (EH_2 form; ref *18*) to −285 mV for Nox (E/EH_2 form); stoichiometric addition of NAD^+ to the Npx EH_4 form gives direct conversion to $EH_2{\cdot}NADH$ (*18*), but the Nox EH_4 subunit only binds NAD^+ tightly to give the charge-transfer complex. Even more significant is the effect of Cys42-S^- on the respective potentials; the C42S Npx flavin potential is increased to −219 mV (+93 mV change; ref *11*) while that for C42S Nox increases only 10 mV (−275 mV). Reduction of Cys42-SOH in Npx and the resulting strong charge-transfer interaction between Cys42-S^- and FAD drive the flavin potential down by almost 100 mV, while the same process in Nox only decreases E'^0 by 10 mV. While the thermodynamic description of these active-site interactions does not fully account for the rapid reduction of Nox EH_2

[3] J. Luba, V. Charrier, and A. Claiborne, *Biochemistry* (in press).

→ EH_4 observed catalytically with NADH, it does provide a framework for distinguishing the respective four-electron versus two-electron redox cycles catalyzed by these enzymes.

REFERENCES

1. Ahmed, S. A., and Claiborne, A. (1989) *J. Biol. Chem 264*, 19856−19863.
2. Ahmed, S. A., and Claiborne, A. (1989) *J. Biol. Chem 264*, 19864−19870.
3. Condon, S. (1987) *FEMS Microbiol. Rev. 46*, 269−280.
4. Higuchi, M. (1992) *Oral Microbiol. Immunol. 7*, 309−314.
5. Higuchi, M., Shimada, M., Yamamoto, Y., Hayashi, T., Koga, T., and Kamio, Y. (1993) *J. Gen. Microbiol. 139*, 2343−2351.
6. Claiborne, A., Crane, E. J., III, Parsonage, D., Yeh, J. I., Hol, W. G. J., and Vervoort, J. (1997) in *Flavins and Flavoproteins 1996* (Stevenson, K. J., Massey, V., and Williams, C. H., Jr., Eds.) pp 731−740, University of Calgary Press, Calgary, AB.
7. Yeh, J. I., Claiborne, A., and Hol, W. G. J. (1996) *Biochemistry 35*, 9951−9957.
8. Crane, E. J., III, Vervoort, J., and Claiborne, A. (1997) *Biochemistry 36*, 8611−8618.
9. Mallett, T. C., and Claiborne, A. (1998) *Biochemistry 37*, 8790−8802.
10. Miller, S. M., Massey, V., Williams, C. H., Jr., Ballou, D. P., and Walsh, C. T. (1991) *Biochemistry 30*, 2600−2612.
11. Parsonage, D., and Claiborne, A. (1995) *Biochemistry 34*, 435−441.
12. Ross, R. P., and Claiborne, A. (1992) *J. Mol. Biol. 227*, 658−671.
13. Parsonage, D., Miller, H., Ross, R. P., and Claiborne, A. (1993) *J. Biol. Chem. 268*, 3161−3167.
14. Ahmed, S. A., and Claiborne, A. (1992) *J. Biol. Chem. 267*, 25822−25829.
15. Parsonage, D., Luba, J., Mallett, T. C., and Claiborne, A. (1998) *J. Biol. Chem. 273*, 23812−23822.
16. Walsh, C., Fisher, J., Spencer, R., Graham, D. W., Ashton, W. T., Brown, J. E., Brown, R. D., and Rogers, E. F. (1978) *Biochemistry 17*, 1942−1951.
17. Leatherbarrow, R. (1987) *Enzfitter*, Biosoft, Hills Road, Cambridge, U.K.
18. Crane, E. J., III, Parsonage, D., Poole, L. B., and Claiborne, A. (1995) *Biochemistry 34*, 14114−14124.
19. Pfleiderer, G., Jeckel, D., and Wieland, T. (1956) *Biochem. Z. 328*, 187−194.
20. Fersht, A. (1985) *Enzyme Structure and Mechanism*, 2nd ed., pp 189−190, W. H. Freeman, New York.
21. Clark, W. M. (1960) *Oxidation−Reduction Potentials of Organic Systems*, Williams & Wilkins Co., Baltimore, MD.
22. Cleland, W. W. (1964) *Biochemistry 3*, 480−482.
23. Dawson, R. M. C., Elliott, D. C., Elliott, W. H., and Jones, K. M. (1986) *Data for Biochemical Research*, 3rd ed., pp 380−381, Clarendon Press, Oxford, U.K.
24. Loach, P. A. (1976) in *Handbook of Biochemistry and Molecular Biology* (Fasman, G. D., Ed.) 3rd ed., Vol. I, pp 122−130, CRC Press, Boca Raton, FL.
25. Fisher, T. L., Vercellotti, S. V., and Anderson, B. M. (1973) *J. Biol. Chem. 248*, 4293−4299.
26. Circular OR-18 (1961) P-L Biochemicals, Inc., Milwaukee, WI.
27. Thorpe, C., and Williams, C. H., Jr. (1981) *Biochemistry 20*, 1507−1513.
28. Mayhew, S. G., Foust, G. P., and Massey, V. (1969) *J. Biol. Chem. 244*, 803−810.
29. Stankovich, M. T., Schopfer, L. M., and Massey, V. (1978) *J. Biol. Chem. 253*, 4971−4979.
30. Ghisla, S., Massey, V., Lhoste, J.-M., and Mayhew, S. G. (1974) *Biochemistry 13*, 589−597.
31. Thorpe, C., and Williams, C. H., Jr. (1976) *J. Biol. Chem. 251*, 7726−7728.
32. Williams, C. H., Jr. (1992) in *Chemistry and Biochemistry of Flavoenzymes* (Müller, F., Ed.) Vol. III, pp 121−211, CRC Press, Boca Raton, FL.
33. Miller, S., Moore, M. J., Massey, V., Williams, C. H., Jr., Distefano, M. D., Ballou, D. P., and Walsh, C. T. (1989) *Biochemistry 28*, 1194−1205.
34. Engst, S., and Miller, S. M. (1998) *Biochemistry 37*, 11496−11507.
35. Schiering, N., Kabsch, W., Moore, M. J., Distefano, M. D., Walsh, C. T., and Pai, E. F. (1991) *Nature 352*, 168−172.
36. delCardayré, S. B., and Davies, J. E. (1998) *J. Biol. Chem. 273*, 5752−5757.
37. Schopfer, L. M., and Massey, V. (1979) *J. Biol. Chem. 254*, 10634−10643.
38. Massey, V., and Palmer, G. (1962) *J. Biol. Chem. 237*, 2347−2358.
39. Matthews, R. G., and Williams, C. H., Jr. (1976) *J. Biol. Chem. 251*, 3956−3964.
40. Mallett, T. C., Parsonage, D., and Claiborne, A. (1997) in *Flavins and Flavoproteins 1996* (Stevenson, K. J., Massey, V., and Williams, C. H., Jr., Eds.) pp 781−784, University of Calgary Press, Calgary, AB.
41. Massey, V. (1994) *J. Biol. Chem. 269*, 22459−22462.
42. Stehle, T., Ahmed, S. A., Claiborne, A., and Schulz, G. E. (1991) *J. Mol. Biol. 221*, 1325−1344.
43. Stehle, T., Claiborne, A., and Schulz, G. E. (1993) *Eur. J. Biochem. 211*, 221−226.

BI9817717